Hydrogen in chondrites: Influence of parent body alteration and 1 atmospheric contamination on primordial components

Lionel G Vacher, Laurette Piani, Thomas Rigaudier, Dorian Thomassin, Maxime Piralla, Yves Marrocchi

Hydrogen in chondrites: Influence of parent body alteration and atmospheric contamination on primordial components

Lionel G. Vacher[1,2*], Laurette Piani[1], Thomas Rigaudier[1], Dorian Thomassin[1], Guillaume Florin[1], Maxime Piralla[1] & Yves Marrocchi[1]

[1]CRPG, CNRS, Université de Lorraine, UMR 7358, Vandoeuvre-lès-Nancy, F-54501, France

[2]Department of Physics, Washington University, St. Louis, St. Louis, MO, USA

[*]Corresponding author: l.vacher@wustl.edu

Abstract

Hydrogen occurs at the near percent level in the most hydrated chondrites (CI and CM) attesting to the presence of water in the asteroid-forming regions. Their H abundances and isotopic signatures are powerful proxies for deciphering the distribution of H in the protoplanetary disk and the origin of Earth's water. Here, we report H contents and isotopic compositions for a set of carbonaceous and ordinary chondrites, including previously analyzed and new samples analyzed after the powdered samples were degassed under vacuum at 120°C for 48 hours to remove adsorbed atmospheric water. By comparing our results to literature data, we reveal that the H budgets of both H-poor and H-rich carbonaceous chondrites are largely affected by atmospheric moisture, and that their precise quantification requires a specific pre-degassing procedure to correct for terrestrial contamination. Our results show that indigenous H contents of CI carbonaceous chondrites usually considered the more hydrated meteorites are almost a factor of 2 lower than those previously reported, with uncontaminated D/H ratios differing significantly from that of Earth's oceans. Without pre-

degassing, the H concentrations of H-poor samples (e.g., CVs chondrites) are also affected by terrestrial contamination. After correction for contamination, it appears that the amount of water in chondrites is not controlled by the matrix modal abundance, suggesting that the different chondritic parent bodies accreted variable amounts of water-ice grains. Our results also imply that (i) thermal metamorphism play an important role in determining the H content of both CV and ordinary chondrites but without affecting drastically their H isotopic composition since no clear D enrichment is observed with the increase of petrographic type and (ii) the D enrichment of ordinary chondrites does not result from the loss of isotopically light H_2 induced by metal oxidation but is rather linked to the persistence of a thermally resistant D-rich component.

1. Introduction

Hydrogen is the most abundant element in the solar system, but is present in only minor to trace amounts in asteroids and planetary bodies. Throughout the solar system and its history, H has occurred in various species, most commonly (i) H_2 in the gas phase, (ii) H_2O molecules mostly as vapor and ice, (iii) OH^- or H_2O in silicate minerals, melts, and glasses, (iv) C-bonded H in organic compounds and (v) minor volatile species, such as NH_3 and H_2S. Today, water is present as ice, vapor, and/or liquid on Earth and other planets, dwarf planets, moons, and comets. The presence of OH^- or H_2O in the silicate minerals comprising primitive meteorites attests to the past existence of water on their asteroidal parent bodies and constitutes an invaluable record of the distribution and composition of water in the protoplanetary disk.

The H isotopic composition of water (expressed as D/H or per-mil deviations relative to Vienna standard mean ocean water, VSMOW, as $\delta D = [(D/H_{sample}/D/H_{VSMOW}) - 1] \times 1000$,

where $D/H_{VSMOW} = 155.76 \times 10^{-6}$) in planetary objects is generally thought to increase with increasing heliocentric distance, from H_2O that was in isotopic exchange with D-poor H_2 near the sun ($D/H \approx 21 \times 10^{-6}$; Geiss and Gloeckler, 2003), to intermediate D/H ratios in inner solar system objects (e.g., Earth's ocean, $D/H \approx 156 \times 10^{-6}$), to D-enriched outer solar system objects such as comets (D/H up to 530×10^{-6} in comet 67P/Churyumov-Gerasimenko; Altwegg et al., 2014). Determining the precise abundances and isotopic compositions of H in meteorites—as representative samples of asteroids—is thus of fundamental importance for understanding the source(s) of water in the asteroid-forming regions (Alexander et al., 2012; Piani et al., 2015, 2018; Piani and Marrocchi, 2018) and potential radial mixing during the evolution of the protoplanetary disk (Vacher et al., 2016; Piani et al., 2018).

The origin of water on Earth and other telluric planets is also a long-standing question (Alexander, 2017; McCubbin and Barnes, 2019). Although it is commonly assumed that the building blocks of the terrestrial planets derived from a cosmochemical reservoir best represented by enstatite chondrites, they accreted in a region where temperatures were too high for water and other volatiles to condense (Albarede, 2009). Therefore, these bodies are expected to be highly volatile-depleted, though they have tenuous atmospheres and water is largely present on Earth and Mars (Taylor, 2013), and possibly in the Venusian and Mercurian atmospheres (Smrekar and Sotin, 2012). For Earth, this paradox is generally bypassed by invoking the late accretion of 1−4 wt% of hydrated carbonaceous chondrites (i.e., CI-CM chondrites), which arrived at Earth due to the formation and subsequent migration of Jupiter (Morbidelli et al., 2000; Marty, 2012; Marty et al., 2016; Raymond and Izidoro, 2017).

Such a conclusion is highly dependent on our ability to precisely quantify the bulk H contents and D/H ratios of extraterrestrial materials. This point is not trivial since, despite being commonly measured, H is the most prone element to terrestrial contamination (except for noble gases; Protin et al., 2016). For instance, it was recently shown that Martian

meteorites suffer rapid (<1 yr) terrestrial weathering and contamination that largely affect the water contents and H isotopic compositions of minerals exposed at their surface (Stephant et al., 2018). Moreover, water and volatile hydrocarbons (CH_2 and CH_3) quickly adsorb onto rock surfaces, raising potential H and C contamination issues during sample preparation (Salisbury et al., 1991). This implies that the H budget estimated for a given meteorite is a complex mixture between indigenous hydrogen in minerals and organics and exogenous H due to terrestrial weathering and adsorption. Corrections for exogenous H could be achieved by performing (i) stepwise heating measurements to decipher between adsorbed, alteration, and indigenous water (Robert and Epstein, 1982; Kerridge, 1985) or (ii) sample degassing under vacuum at low temperature (e.g., Vacher et al., 2016). Bulk H budget reconstructions from stepwise heating experiments are difficult due to the presence of different water-bearing minerals characterized by variable contamination susceptibilities that release adsorbed water at various temperatures. Furthermore, there is no consensus on a procedure to remove adsorbed water from both terrestrial and extraterrestrial materials, and different studies have employed various temperatures (70–350 °C) and durations (2–480 h) of heating under vacuum (Savin and Epstein, 1970; Girard et al., 2000; Gong et al., 2007; Lupker et al., 2012). Of note, a recent estimation of the bulk H contents and isotopic compositions of a large set of chondrites was performed without a pre-degassing protocol (Alexander et al., 2012), and therefore may have overestimated the H budget of primitive meteorites. In addition to terrestrial contamination, meteorites experienced parent-body alteration processes (hydrothermal alteration and thermal metamorphism; Brearley, 2006; Huss et al., 2006; Marrocchi et al., 2018) whose influence on their pre-accretion H characteristics remains unclear.

Here, to better understand the origin of hydrogen accreted by chondrites, we report the H concentrations and isotopic compositions of a large set of carbonaceous and ordinary

chondrites. To test the influence of laboratory pre-degassing temperature, we selected chondrites that have been previously characterized (C2-ung. = Tagish Lake; CI = Orgueil and Alais; CY = Yamato 980115; King et al., 2019a; CM = Murchison, Mighei, and Murray; CV = Allende, Bali, Grosnaja, Kaba, and Vigarano; Robert and Epstein, 1982; Kerridge, 1985; Pearson et al., 2001; Alexander et al., 2012). As CM chondrites represent 25% of all carbonaceous chondrite falls (Gounelle et al., 2005), several new CMs have recently been described. We thus report the H concentrations and isotopic compositions of new CM falls (Aguas Zarcas, Maribo and Munkundpura; Haack et al., 2012; Rudraswami et al., 2019) and finds (Lonewolf Nunataks (LON) 94101 and Jbilet Winselwan; Lindgren et al., 2013; King et al., 2019b). In addition, several ordinary chondrites and a CK-type carbonaceous chondrite covering the entire range of thermal metamorphism (Tait et al., 2014) were analyzed to test the influence of parent-body metamorphism on H characteristics (L3 = Grosvenor Mountains (GRO) 95502, CK4 = Karoonda, L4 = Saratov, LL/L4 = Bjurbole, H4 = Sainte Marguerite, and H6 = Kernouve). We use our results to discuss the nature of primordial components accreted by chondrites and the influence of post-accretion effects, either in asteroidal bodies or at Earth's surface.

2. Materials and method

2.1 Bulk measurements of H contents and isotope compositions

Hydrogen concentrations, [H], and isotopic compositions, D/H, of the different meteoritic samples were determined on-line using the Thermo Scientific EA IsoLink - deltaV IRMS System at CRPG laboratory (Nancy, France) according to the procedure developed by Lupker et al. (2012). First, meteoritic samples were crushed into powder in an agate mortar, weighed in tin capsules (CM, CI, CY and Tagish Lake: 1–3 mg; CV, CK, and OC: 4–10 mg), and the samples and capsules were loaded into a sample carrousel and degassed under vacuum at 120 °C for 48 h in a degassing canister (Lupker et al., 2012; Gaudin et al., 2015; Fig. 1A); degassing for less than 48 h was shown to result in increased variability of water contents and isotopic compositions due to remaining absorbed water (Lupker et al., 2012). After dehydration, the degassing canister was opened in a dry, N_2-flushed glove box and the sample carrousel was transferred into a sealed auto-sampler initially pre-flushed with He (Fig. 1B). The auto-sampler was then connected to the EA and pumped out during 20 min before opening it to the reduction column as a precautionary step to suppress any potential rehydration of the samples in the event of atmospheric contact between degassing and analysis.

The samples were combusted at 1450 °C (required temperature to ensure rapid sample reduction and to prevent any CH_3 formation) on a glassy carbon reaction tube filled with glassy carbon chips and itself placed into a ceramic liner to reduce hydroxyls (OH) released by the samples into H_2 according to the reaction: $2OH + C \text{ (unlimited in reactor)} \rightarrow 2CO + H_2$ (Fig. 1C). The produced gases were separated on a chromatographic column maintained at 60 °C and the extracted H_2 was introduced into the mass spectrometer through an open-split and

its D/H isotopic composition was analyzed (Fig. 1D). The extracted H_2 was corrected for H_3^+ contributions using in-house H_2 standard injections and [H] and D/H were determined by comparison with seven internal standards routinely included during the analyses: (i) phlogopite (Mica-Mg, 0.29 wt.% H, D/H = 143.8×10^{-6}), (ii) muscovite (MuscD65, 0.474 wt.% H, D/H = 142.6×10^{-6}), (iii) a fine-grained marine sediment from the Bay of Bengal (SO188, 0.489 wt.% H, D/H = 142.7×10^{-6}), and (iv) four basalts with different H concentrations (CYP78, 0.14 wt.% H; JB3-GSJ, 0.20 wt.% H; SR2-02, 0.27 wt.% H; and GMR-KS12, 0.42 wt.% H). Errors on hydrogen concentrations, calculated as twice the standard deviation divided by the average, increase with decreasing standard water content following the negative power law $2SD / [H] = 0.05 \times [H]^{-0.43}$, which was used to estimate the 2σ sample errors reported in Table 1. Hydrogen isotopic compositions are reported as D/H ratios or as δD values (‰) relative to VSMOW. The reproducibility of this method is better than 15% (2σ) for [H] and 0.5×10^{-6} for D/H (or 5‰ for δD).

2.2 Bulk measurements of C and N concentration and isotopic compositions

Carbon and nitrogen concentrations ([C] and [N], respectively) and carbon isotopic compositions ($\delta^{13}C$, $^{13}C/^{12}C$ variations reported relative to Vienna Pee Dee Belemnite, VPDB, where $^{13}C/^{12}C_{VPDB} = 0.01123720$) of the different meteoritic samples were determined on-line using the Thermo Scientific EA IsoLink - deltaV IRMS System at the CRPG laboratory. Samples were crushed into fine powder and wrapped in tin capsules (2–29 mg). The capsules were loaded in a specific auto-sampler connected to the EA and pumped out during 20 min before opening it to the oxidation column. Samples were then introduced into an oxidation reactor made of a quartz tube filled with chromium oxide, pure copper, and silvered cobalt oxide and heated at 1020 °C. A controlled pulse of oxygen causes the oxidation of tin

capsules leading to an exothermic reaction that raises the sample temperature to about 1800°C. The produced gases (N_2, CO_2) were separated on a chromatographic column maintained at 70 °C and the carbon isotopic composition of the extracted CO_2 was measured with a Thermo Scientific Delta V Advantage continuous flow IRMS. Carbon isotopic composition were determined by comparison with two internal and two international standards routinely included during the analysis: (i) BFSd ($\delta^{13}C$ = -21.5‰), (ii) CRPG_M2 ($\delta^{13}C$ = -24.98‰), (iii) NBS22 ($\delta^{13}C$ = -30.03‰) and (iv) USGS24 ($\delta^{13}C$ = -16.1‰). Values are quoted in the delta notation in ‰ relative to V-PDB and the reproducibility was better than 0.2‰. Four internal standards were used to calculate [N] and [C]: (i) BFSd (0.53 wt.% C), (ii) CRPG_M2 (0.408 wt.% C), (iii) Eurovector Synthetic Soil Mix #1 (0.216 wt.% N, 3.5 wt.% C) and (iv) Eurovector Synthetic Soil Mix #4 (0.048 wt.% N, 2.417 wt.% C). Errors (2σ) on [N] are estimated to be 10% and 30% for samples containing more and less than 0.08 wt.% N, respectively. For carbon analyses, 2σ errors are expected to be 2% for [C] and 2‰ for $\delta^{13}C$.

3. Results

3.1 Hydrogen characteristics of chondrites

Results from hydrogen extractions and associated D/H isotopic analyses are presented in Table 1 and Figure 2. For most samples (excluding C2-ung. Tagish Lake and CI Alais for their D/H variability), replicate aliquots of the same meteorite exhibit good reproducibility, with 2σ standard deviations less than 15% for [H] and 5‰ for δD.

Hydrogen abundances of CI, CY and CM chondrites vary widely, but exhibit comparable ranges, from 0.47 to 1.01 wt.% H (Fig. 2A). The lowest hydrogen contents were measured in CM Jbilet Winselwan, possibly due to dehydration during parent-body metamorphism (King et al., 2019b). CMs are depleted in deuterium compared to CIs (D/H_{CM} = 131–170 × 10^{-6} *vs.* $D/H_{CI} \approx 177 \times 10^{-6}$) but show similar range of D/H values as the CY Antarctica Y-980115 (D/H_{CY} = 139 × 10^{-6}, Fig. 2B). The low hydrogen content of Y-980115 (0.71 wt.% H) relative to CI-CM chondrites and its D-poor isotopic composition might be might be a consequence of (i) thermal metamorphosed at temperature > 500°C (King et al., 2019a) and/or (ii) terrestrial weathering (e.g., Alexander et al., 2018a). The ungrouped C2 carbonaceous chondrite Tagish Lake exhibits a hydrogen content similar to the lowest value measured for CM chondrites (0.43 wt.% H), but this unique carbonaceous chondrite is the most D enriched (D/H = 225 × 10^{-6}, Fig. 2A and B), consistent with previous measurements (Pearson et al., 2001; Alexander et al., 2012). CV chondrites (0.06–0.19 wt% H, Fig. 2A) contain lower hydrogen concentrations than CM and CI chondrites, whereas their hydrogen isotopic compositions are highly variable (D/H = 139–161 × 10^{-6}, Table 1) over a range similar to that of CM chondrites (Fig. 2B). Ordinary chondrites and CK-type carbonaceous chondrites present the lowest hydrogen concentrations (≤0.03 wt.% H, excluding Grosvenor

Mountains (GRO) 95502, an Antarctic find possibly affected by terrestrial weathering; Fig. 2A), and have relatively D-poor hydrogen isotopic compositions (D/H = 134–144 × 10^{-6}, Fig. 2B).

3.2 Nitrogen and carbon characteristics of chondrites

Table 2 summarizes the carbon and nitrogen contents and carbon isotopic compositions of the analyzed chondrites. CI, CY and CM chondrites contain the highest N and C contents in this study, with 0.09–0.17 wt.% N and 1.54–3.04 wt.% C in CMs and 0.09–0.21 wt.% N and 3.06–3.35 wt.% C in CIs (Fig. 3). They both show comparable ranges of carbon isotopic compositions, with $\delta^{13}C$ ranging from –16 to –13‰ and –14 to –4‰ for CIs and CMs, respectively. The nitrogen and carbon concentrations in Tagish Lake (0.11 wt.% N and 2.14 wt.% C) are comparable to those in CM chondrites, but with a more ^{13}C-enriched isotopic composition ($\delta^{13}C \approx +5$‰). Compared with these C- and N-rich chondrites, CV, CK, and ordinary chondrites are depleted in N (≤0.03 wt.%) and C (≤1.42 wt.%), and have lower carbon isotopic compositions than hydrated chondrites, with $\delta^{13}C \approx -27$ to –18‰.

4. Discussion

4.1 Effect of terrestrial contamination in carbonaceous chondrites

4.1.1 Influence of pre-degassing temperature on the total H budget

Immediately after falling to Earth's surface, meteorites are exposed to terrestrial moisture and precipitation that could significantly affect their H characteristics, even in dry environments such as hot deserts (Stephant et al., 2018). Consequently, bulk meteorite H budgets are complex mixtures of indigenous hydrogen, terrestrial weathering, and adsorbed water hosted by different minerals/phases with variable thermal behaviors. Thermogravimetric analysis and derivate curves obtained in the range 25–1200 °C (Garenne et al., 2014; King et al., 2015; Gilmour et al., 2019) suggest a complex thermal evolution of H-bearing phases with the following release temperatures: (i) 25–200 °C for absorbed H_2O, (ii) 200–400 °C for water in hydroxides and H-bearing organic matter, (iii) 400–770 °C for OH^- in phyllosilicates, and (iv) 770–900 °C for H_2O in sulfates. Although suspected to occur to some degree at 200–400 °C, it has been proposed that adsorbed terrestrial water is mainly released from hydrated carbonaceous chondrites at 25–250 °C (Boato, 1954; Kerridge, 1985; Baker et al., 2002; Garenne et al., 2014; Gilmour et al., 2019).

Alexander et al. (2012, 2013) reported H concentrations and isotopic compositions for a large set of carbonaceous chondrites that were stored in desiccators at room temperature for days to weeks prior to analyses. Their data define a positive correlation in a D/H *vs.* 1/H diagram (Fig. 4) that reveals the increasing contribution of H-bearing, D-rich, insoluble organic matter (IOM; Alexander et al., 2007; Alexander et al., 2012) to the total H budget, the largest contributions coming from phyllosilicates in hydrated chondrites. Our data define a

similar positive trend, but with a statistically different slope (Fig. 4) that reveals the influence of the pre-degassing temperature on observed meteorite H features. Thereby, our bulk H measurements of samples also measured by Alexander et al. (2012) demonstrate that pre-degassed CM and CI chondrites contain ~10–30% and ~40% less H, respectively, than non-degassed samples (Fig. 4). Several reasons can be invoked to explain such important differences: (i) the significant loss of indigenous hydrogen induced by the pre-degassing protocol, leading to an underestimated H budget, (ii) sample heterogeneity, the effects of which are apparent due to the small amounts of material analyzed, and/or (iii) the intended removal of absorbed terrestrial water.

To test these different scenarios, we estimated the H isotopic composition of the hydrogen lost during pre-degassing at 120 °C for 48 h using the following mass balance equation:

$$[\mathrm{H}]_{\mathrm{lost}} \times \mathrm{D/H}_{\mathrm{lost}} = [\mathrm{H}]_{25\,^{\circ}\mathrm{C}} \times \mathrm{D/H}_{25\,^{\circ}\mathrm{C}} - [\mathrm{H}]_{120\,^{\circ}\mathrm{C}} \times \mathrm{D/H}_{120\,^{\circ}\mathrm{C}} \quad (1)$$

where $[\mathrm{H}]_{25\,^{\circ}\mathrm{C}}$, $[\mathrm{H}]_{120\,^{\circ}\mathrm{C}}$, $\mathrm{D/H}_{25\,^{\circ}\mathrm{C}}$, and $\mathrm{D/H}_{120\,^{\circ}\mathrm{C}}$ correspond to the bulk H concentrations and isotopic compositions of the samples determined at room temperature (i.e., 25 °C) and after pre-degassing at 120 °C for 48 h, respectively. The hydrogen lost during pre-degassing corresponds to $[\mathrm{H}]_{\mathrm{lost}} = [\mathrm{H}]_{25\,^{\circ}\mathrm{C}} - [\mathrm{H}]_{120\,^{\circ}\mathrm{C}}$. Consequently, if the H lost during pre-degassing was adsorbed terrestrial water, its calculated H isotopic composition should be (i) similar from one sample to the next and (ii) within the range of terrestrial values. On the other hand, large H isotopic variations are expected if the H lost resulted from sample heterogeneity or the removal of indigenous hydrogen. The H isotopic compositions of pre-degassed H range from D/H ~ 150–155 × 10^{-6} for Murchison, Mighei, Murray, and Orgueil. These values are in the range of H isotopic ratios reported for terrestrial hydrosphere reservoirs (115–165 × 10^{-6};

293 Lécuyer et al., 1998; Frankenberg et al., 2009; Clog et al., 2013), but differ strongly from the
294 (i) D-poor phyllosilicates that bear the signature of asteroidal water in CM and CI chondrites
295 (D/H ~ 85–125 × 10^{-6}; Alexander et al., 2012; Piani et al., 2018, 2019) and (ii) D-rich organic
296 matter (D/H ~ 265–310 × 10^{-6}; Alexander et al., 2007). Consequently, we interpret the
297 differences in H concentrations obtained with and without the pre-degassing routine as mostly
298 due to contamination of primitive meteorites by atmospheric moisture. This scenario cannot,
299 however, explain the D/H ratio calculated of the H degassed from LON 94101, which display
300 a significantly higher D/H value compared to the other common samples (~ 400 × 10^{-6}). By
301 analogy with other CM chondrites, the removal of indigenous H during pre-degassing would
302 result in a D-poor signature for $[H]_{lost}$, at odds with our calculations. Alternatively, the
303 preferential degassing of H from D-rich IOM or H-bearing organic compounds (i.e., small
304 hydrocarbons or molecules found in the soluble part of the meteoritic organic matter) might
305 explain such high D/H values and contributed to the H budget removed during our pre-
306 degassing procedure. However, given that (i) the H isotopic compositions of $[H]_{lost}$ are D-poor
307 compared to organic molecules in carbonaceous chondrites (Pizzarello et al., 1994; 2006;
308 Yamashita & Naraoka, 2014), (ii) stepwise pyrolysis performed by Robert and Epstein (1982)
309 on Murchison and Murray indicates that only few amount of carbon (~ 0.2 mol% of the total
310 C) were lost compared to water below 200 °C (11.5 and 10.8 mol% of the total H,
311 respectively), and (iii) the decomposition of IOM likely occurs at 200–500 °C (Gilmour et al.,
312 2019; Remusat et al., 2019), we concluded that the amount of indigenous organics volatile
313 lost during pre-degassing is not significant and the D-rich compositions of the $[H]_{lost}$ by LON
314 94101 is rather a consequence of sample heterogeneity (Lindgren et al., 2013).
315

316 4.1.2 Quantification of terrestrial contamination in carbonaceous chondrites

317

318 To estimate the influence of pre-degassing, we compare hydrogen concentrations and
319 isotopic compositions measured in different studies for CI Orgueil and CM Murchison as a
320 function of pre-degassing temperature. Murchison shows ~30% less H after pre-degassing at
321 200 °C compared to measurements performed without pre-degassing (Fig. 5A–C).
322 Isotopically, this sample does not show a large change, with D/H value of ~150 × 10^{-6} (Fig.
323 5C). In contrast, a sample of Orgueil pre-degassed at 120–350 °C shows (i) a H loss of up to
324 ~40–80% and (ii) a D/H increase up to ~190 × 10^{-6} relative to samples measured without pre-
325 degassing (D/H ~ 150 × 10^{-6}; Figs. 5B–D). This disparity between CM and CI chondrites
326 probably derives from the fact that the bulk D/H values of CMs, which result from the
327 combined contributions of D-poor water and D-rich OM, are fortuitously close to the D/H
328 values imparted by atmospheric contamination (D/H_{CM} ~ 142 × 10^{-6} *vs.* $D/H_{[H]\,lost}$ ~ 150 × 10^{-6}), and contamination thus produces only minor changes. In contrast, water and OM in CIs are
329
330 D-rich compared to CMs (Busemann et al., 2006; Alexander et al., 2007; Piani et al., 2018,
331 2019), with bulk H isotopic compositions (D/H_{CI} ~ 177 × 10^{-6}) markedly higher than that of
332 the contaminating water. Consequently, the effects of atmospheric moisture are more
333 perceptible in CIs than in CMs.

334 To better quantify the influence of terrestrial contamination, we compared $[H]_{lost}$ (=
335 $[H]_{25\,°C} - [H]_{120\,°C}$) for different chondrites as a function of the H concentration determined
336 after pre-degassing at 120°C. We thusly obtained separate linear trends for CI, CM and CV
337 carbonaceous chondrites, indicating that meteorites containing more H are more prone to
338 contamination (Fig. 6). Interestingly, CM- and CI-type chondrites seem to define a single
339 trend (r^2 = 0.70; MSWD = 1.5), suggesting that CIs would be more affected by H
340 contamination than CMs (Fig. 6). The H concentrations of Tagish Lake are highly

heterogeneous (H = 1.37 and 0.85 wt.%, from Pearson et al., 2001, and Alexander et al., 2012, respectively) and have been shown to depend strongly on the studied lithology (H = 0.74–0.94 wt.%; Alexander et al., 2012); however, as we do not have the petrological details of the Tagish lake pieces measured in our study, we omit Tagish Lake from further discussion.

The difference in the amount of H loss between CI and CMs probably reflects secondary mineralogical diversity between these two groups of chondrites (Fig. 6). CI chondrites are mainly dominated by serpentine and saponite minerals, the latter being clay minerals with the capacity to absorb significant amounts of water into their inter-layers (Tomeoka and Buseck, 1988; King et al., 2015). Thus, it is likely that CI chondrites contains indigenous inter-layer water that could be removed alongside with terrestrial water during pre-degassing, leading to an underestimation of the H budget in CI chondrites. Nevertheless, it appears that the high abundance of inter-layer water in Orgueil is probably related to its long residence time on Earth (since 1864) and it is likely that this meteorite was devoid of inter-layer water prior to its arrival on Earth (Baker et al., 2002). In addition, stepwise heating performed on Orgueil demonstrated that water released at temperature lower than 200 °C is characterized by terrestrial-like values (i.e., $\Delta^{17}O$ = 0 ‰ and D/H = 153 × 10^{-6}), supporting that only minor indigenous water was present in the inter-layers of Orgueil (Robert and Epstein, 1982; Baker et al., 2002). In contrast, CM chondrites are almost saponite-free, and are instead dominated by Fe-Mg-rich serpentine that retains less absorbed water in its silicate layers than saponite (Barber 1981; Howard et al., 2015). It is unclear why the CV trend is separate from the CI-CM trend, but the amount of H lost during pre-degassing suggests that this group of chondrites is also very sensitive to terrestrial alteration and can absorb similar H proportions as CM chondrites (Fig. 6). Phyllosilicates are modally less abundant in CV (up to 4 vol.%; Howard et al., 2010) than in CM chondrites (~75 vol.%; Howard et al., 2015).

Assuming that phyllosilicates are the main storage sites for atmospheric moisture in hydrated carbonaceous chondrites, water adsorption should be vastly lower in CV than in CM chondrites (even accounting for the mineralogical differences of their phyllosilicates). Alternatively, CI and CM phyllosilicates are almost water saturated—i.e., their water adsorption capacity is limited—whereas CV phyllosilicates, despite being less abundant, have more adsorption sites available for accommodating atmospheric moisture. Whatever the reason, it is apparent that terrestrial contamination can greatly affect the H budgets of the most H-poor (CV-like) and H-rich (CI-like) chondrites alike (Figs. 5 and 6). The bulk H contents and D/H ratios of chondrites should thus be measured after pre-degassing under vacuum at ≥120 °C. The consequences of correcting the H compositions of chondrites for terrestrial contamination are discussed in §4.3.

4.2 The influence of thermal metamorphism

4.2.1 CV-type carbonaceous chondrites

CV chondrites are divided into three subgroups partly reflecting their various aqueous and thermal alteration histories: reduced, CV_{Red}; oxidized Allende-like, CV_{OxA}; and oxidized Bali-like, CV_{OxB}. Of the oxidized CVs, the CV_{OxB} subgroup is the most extensively altered and contains abundant phyllosilicates and chondrules replaced by phyllosilicates and magnetite. In contrast, the CV_{OxA} and CV_{Red} subgroups contain minor phyllosilicates and abundant Ca-Fe-rich secondary phases such as andradite, hedenbergite, and kirschsteinite (Krot et al., 2004; Brearley, 2006; Howard et al., 2010; Ganino and Libourel, 2017). CV3s have experienced various degrees of metamorphism that are partly overprinted by subsequent aqueous alteration and further obscured by brecciation (Bonal et al., 2006). Based on the

maturation grade of their organic matter, Bonal et al. (2006) assigned a range of petrographic degrees for the CV chondrites Kaba (~3.1), Vigarano (3.1–3.4), Bali and Grosnaja (~3.6), and Allende (>3.6), although they highlighted the occurrence of clasts of different petrologic types within individual meteorites (e.g., Bali). The H-, C-, and N-concentrations and isotopic compositions measured for these CV chondrites reflect the complex inputs of brecciation and aqueous and thermal alteration, with no clear behavior of these elements and isotopes with increasing petrologic type (Figs. 6 and 7a; Tables 1 and 2). Nevertheless, the most metamorphosed CV_{OxA}, Allende, presents the lowest H concentrations, with its most H-depleted lithologies (Yang and Epstein, 1983) having similar H contents as the metamorphosed CK4 Karoonda (Fig. 7a). This result suggests that thermal metamorphism of CV chondrites could induce a significant H loss for petrologic types >3.6 (Fig. 7a).

4.2.2 Ordinary chondrites

Ordinary chondrites (OCs) from the H, L, and LL groups exhibit pervasive imprints of thermal metamorphism and, to a lesser degree, aqueous alteration. Semarkona (LL3.00) and Bishunpur (LL3.15) are among the rare unequilibrated OCs to contain hydrated minerals (smectites) and other secondary phases (calcites) thought to have formed on their parent body from an oxidizing fluid (Alexander et al., 1989). Water measured in these chondrites is enriched in D, as attested by (i) their bulk D/H values up to 600×10^{-6} (McNaughton et al., 1982; Yang and Epstein, 1983) and (ii) *in-situ* measurements of D/H values up to 1800×10^{-6} (Deloule and Robert, 1995; Piani et al., 2015). Such high D enrichments were interpreted either as inherited from the accretion of D-rich ice that originated in cold regions of the solar system (Deloule and Robert, 1995; Piani et al., 2015) or as the result of parent-body processes (Alexander et al., 2012). Bleached chondrules found in LL3, L3, and more rarely in H3

chondrites attest that aqueous alteration was widespread in OCs, but was mostly erased by subsequent thermal metamorphism (Grossman et al., 2000). This later metamorphic event resulted in high degrees of equilibration of the three OC sub-groups spanning petrological types 3–7 and equilibration temperatures up to 1000 °C (Tait et al., 2014).

The five OCs measured herein span the range of H concentrations reported in OCs, with the most metamorphosed chondrites (H6 Kernouve) being the most depleted in hydrogen (Fig. 7B). These five OCs exhibit D/H ratios similar to those previously measured in equilibrated ordinary chondrites (~130–160 × 10^{-6}), and we observe no strong differences between groups or petrological types (Fig. 7B). Furthermore, we do not observe D enrichments with increased parent-body thermal metamorphism (Fig. 7B), in agreement with previous observations (Robert et al., 1979; McNaughton et al., 1982). This is at odds with the assumption that water in ordinary chondrites became increasingly enriched in deuterium due to the oxidation of iron and subsequent loss of isotopically light H_2 (Alexander et al., 2010, 2012; Sutton et al., 2017). This assumption was initially proposed to explain the deuterium enrichment of IOM in OCs with increasing degree of metamorphism, the organic matter thereby being enriched by isotopic exchange with the remaining D-rich water (Alexander et al., 2010). However, given that both the remaining water and OM should have been enriched in D by this process, the bulk D/H ratios of OCs should increase with increasing degree of thermal metamorphism. The absence of such D enrichments in the bulk chondrites thus contradicts the implication of water in the D enrichment of the OM, instead supporting the proposal that ordinary chondrites contain a thermally recalcitrant D-rich organic matter component (Remusat et al., 2016). Overall, thermal metamorphism in OCs seems to have mainly decreased the bulk-rock hydrogen contents without strongly influencing the hydrogen isotopic ratios for petrological types ≥3.2 (Fig. 7B).

The percentage of fayalite (%Fa) in ordinary chondrites increases from H to L to LL groups and is considered a robust proxy of the degree of hydration (i.e., the water content) of their respective parent bodies (Rubin, 2005; Florin et al., 2020). However, the lack of variation between the H contents of the different groups of OCs (Fig. 7B) suggests that they could have accreted similar amounts of water. This could be interpreted as evidence for pre-accretion hydration processes in different regions of the protoplanetary disk. Whereas there is no clear limit between the H contents of unequilibrated and equilibrated OCs, the observed decrease in H contents with increasing metamorphism is in line with the progressive increase of %Fa and the loss of Fe-Ni metal during metamorphism (Florin et al., 2020).

450 4.3 Implication for the origin and abundance of H in chondrites

451

452 Our data suggest that terrestrial contamination can represent a significant part of the
453 measured chondritic H budget, which strongly depends on the analytical protocol and
454 particularly the pre-degassing procedure. The effects of terrestrial contamination are
455 especially important for chondrites with the highest indigenous hydrogen contents within a
456 given chondrite group (Figs. 4 and 6). However, within errors, we observe similar positive
457 correlations and zero intercepts (D/H ~ 100 × 10^{-6} or δD ~ –400‰) between D/H and C/H for
458 CMs (Fig. 8) as previously reported (Alexander et al., 2012). These values represent the
459 isotopic composition of water accreted by the CM parent body (Alexander et al., 2012). This
460 similarity indicates that previous estimations of the D/H ratios of water in the region of CM
461 parent-body accretion (Alexander et al., 2012) were not significantly affected by terrestrial
462 contamination, as also attested by the consistency with *in-situ* measurements via secondary
463 ion mass spectrometry (SIMS; Piani et al., 2018). The D/H ratio of water accreted by CV
464 chondrites was only estimated recently from SIMS measurements (Piani and Marrocchi,
465 2018), and our bulk data confirm their observation that CV water is enriched in deuterium
466 compared to CM water (Fig. 8). If CMs and CVs accreted beyond the orbit of Jupiter as
467 commonly proposed (Kruijer et al., 2017; Nanne et al., 2019), this suggests the existence of
468 different water-ice reservoirs, with CV water being enriched in heavy H and O isotopes (Piani
469 et al., 2018; Piani and Marrocchi, 2018; Marrocchi et al., 2018).

470 Among chondrites, CIs are of primary importance as their bulk chemical compositions
471 are similar to that of the solar photosphere, which is representative of the average solar system
472 composition (Lodders, 2003). In addition, CIs are generally considered to be the most
473 hydrated chondrites based on previous H measurements (Pearson et al., 2001; Alexander et
474 al., 2012) and their high abundances of secondary minerals (~ 97%; King et al., 2015).

Although it remains a possibility that a small amount of the released water below 120°C could have been initially indigenous, our data reveal that CIs analyzed without pre-degassing are essentially contaminated by terrestrial moisture, and we estimate their indigenous water contents to be almost a factor of 2 lower than previously reported (0.93 wt.% H compared to 1.56 wt.% H; Pearson et al., 2001; Alexander et al., 2012), in agreement with results from stepwise heating analyses (Boato, 1954; Robert and Epstein, 1982; Yang and Epstein, 1983; Kerridge, 1985; Eiler and Kitchen, 2004). Consequently, CI chondrites have indigenous water contents similar to those estimated for CM chondrites, suggesting that CIs and CMs accreted similar proportions of water, although they contain vastly different proportions of matrix (65 vol.% and 100 vol.% in CMs and CIs, respectively; Alexander et al., 2018b and references therein). CV chondrites comprising 40 vol.% matrix have H abundances roughly one tenth those of CM and CI chondrites. Together, our results for CV-, CM-, and CI-type carbonaceous chondrites argue against the suggested dependency of the bulk H concentration on matrix content (Alexander et al., 2018b). Nevertheless, our data for C and N concentrations (Fig. 3) are consistent with a matrix content dependency for these elements (Alexander et al., 2018b). Furthermore, correcting for terrestrial water contamination in CIs largely affects their D/H isotopic compositions, which is not the case for CMs (Fig. 5). This implies that CIs do not have H isotopic ratios as close to that of Earth's water as previously estimated based on measurements performed without pre-degassing. This conclusion was reported nearly 40 years ago (Robert and Epstein, 1982; Kerridge, 1985), but was overshadowed by recent studies that did not quantify the effects of terrestrial contamination (Alexander et al., 2012). Consequently, the large contamination of CI water and its non-terrestrial H isotopic composition should be accounted for in models of Earth's formation based on the mixing of chondrite-like materials, as considering CIs as the putative source of Earth's oceans would also affect the ^{54}Cr mass balance calculation (Warren, 2011; Dauphas,

2017). In such a framework, CM chondrites thus appear to be the most isotopically similar extraterrestrial materials to the Earth's surficial hydrogen reservoir.

5. Conclusions

We have determined the bulk hydrogen concentrations and isotopic compositions of a large set of chondritic samples (CI, CM, CV, CK, and ordinary chondrites) using an elemental analyzer coupled to an isotope ratio mass spectrometer. Samples were pre-degassed under vacuum at 120 °C for 48 h before measurements. Our main results are:

1) CI and CM chondrites and Tagish Lake define a correlation in a D/H *vs.* 1/H diagram induced by the increasing contribution of insoluble organic matter to the total H budget. This trend is statistically distinct from that defined by similar chondrites analyzed without pre-degassing at ≥120 °C.

2) No clear D enrichment is observed with the increase of parent-body thermal metamorphism for ordinary and CV-type carbonaceous chondrites.

From these results, we drew the following conclusions:

1) Chondrites are largely affected by terrestrial contamination, with the most hydrated CI chondrites being the most prone to contamination because phyllosilicates are more abundant in CIs compared to CMs and CVs. After correction of contamination, the primordial H contents of CI, CM, and CV chondrites are significantly lower than generally reported and is not related to their matrix modal abundance, implying that their respective parent bodies accreted variable amounts of water-ice grains.

2) The D/H ratio of Orgueil is affected by terrestrial contamination, leading to an important underestimation of its H isotopic composition. This result is important as it could

affects the amount of water delivery by CI chondrites in the models of Earth's formation based on the mixing of chondrite-like materials.

3) Although based on a limited number of samples, thermal metamorphism suggests that significant H were lost in CVs of petrological type >3.6. It also decreased the H contents of ordinary chondrites, but minimally affected the D/H ratios of OCs of petrological type ≥3.2.

4) The absence of an increasing D/H ratio with increasing the metamorphism degree for bulk ordinary chondrites does not support models in which water became enriched in deuterium via the oxidation of iron and the loss of isotopically light H_2. On the contrary, this observation supports the presence of thermally resistant D-rich organic matter in ordinary chondrites.

Acknowledgments

We thank Mike Zolensky and Bernard Marty for providing samples. We also thank the National Institute of Polar Research (Japan), the Natural History Museum of Denmark (Copenhagen), the Muséum national d'Histoire naturelle (Paris, France), the Natural History Museum of Vienna (Austria), and the Antarctic Search for Meteorites (ANSMET) program for loaning samples. US Antarctic meteorite samples were recovered by ANSMET, funded by NSF and NASA, and characterized and curated by the Department of Mineral Sciences of the Smithsonian Institution and Astromaterials Curation Office at NASA Johnson Space Center. This work was funded by l'Agence Nationale de la Recherche through grant ANR-14-CE33-0002-01 SAPINS (PI Yves Marrocchi) and ANR-19-CE31-0027-01 HYDRaTE (PI Laurette Piani) and by the European Research Council (PHOTONIS project, grant agreement No. 695618 to Bernard Marty). This is a CRPG contribution #2728.

Research data

Original data of this study are available in the supplementary file.

References

Albarede F. (2009) Volatile accretion history of the terrestrial planets and dynamic implications. *Nature* **461**, 1227–1233.

Alexander C. M. O.'D. (2017) The origin of inner Solar System water. *Philosophical Transactions of the Royal Society A: Mathematical, Physical and Engineering Sciences* **375**, 20150384–20.

Alexander C. M. O.'D., Barber D. J. and Hutchison R. (1989) The microstructure of Semarkona and Bishunpur. *Geochim. Cosmochim. Acta* **53**, 3045–3057.

Alexander C. M. O.'D., Bowden R., Fogel M. L., Howard K. T., Herd C. D. K. and Nittler L. R. (2012) The Provenances of Asteroids, and Their Contributions to the Volatile Inventories of the Terrestrial Planets. *Science* **337**, 721–723.

Alexander C. M. O.'D., Fogel M., Yabuta H. and Cody G. D. (2007) The origin and evolution of chondrites recorded in the elemental and isotopic compositions of their macromolecular organic matter. *Geochim. Cosmochim. Acta* **71**, 4380–4403.

Alexander C. M. O.'D., Howard K. T., Bowden R. and Fogel M. L. (2013) The classification of CM and CR chondrites using bulk H, C and N abundances and isotopic compositions. *Geochim. Cosmochim. Acta* **123**, 244–260.

Alexander, C. M. O'D., Greenwood, R. C., Bowden, R., Gibson, J. M., Howard, K. T., Franchi, I. A. (2018a). A mutli-technique search for the most primitive CO chondrites. *Geochim. Cosmochim. Acta* **221**, 406–420.

Alexander C. M. O.'D., McKeegan K. D. and Altwegg K. (2018b) Water Reservoirs in Small Planetary Bodies: Meteorites, Asteroids, and Comets. *Space Sci Rev*, 1–47.

Alexander C. M. O.'D., Newsome S. D. and Fogel M. L. (2010) Deuterium enrichments in chondritic macromolecular material—Implications for the origin and evolution of organics, water and asteroids. *Geochim. Cosmochim. Acta* **74**, 4417–4437.

599 Altwegg K. et al. (2014) 67P/Churyumov-Gerasimenko, a Jupiter family comet with a high
600 D/H ratio. *Science* **347**, 1261952–1261952.
601 Barber, D. J. (1981) Matrix phyllosilicates and associated minerals in C2M carbonaceous
602 chondrites. *Geochim. Cosmochim. Acta* ***45***, 945−970.
603 Baker L., Franchi I. A., Wright I. P. and Pillinger C. T. (2002) The oxygen isotopic
604 composition of water from Tagish Lake: Its relationship to low-temperature phases and to
605 other carbonaceous chondrites. *Meteorit. Planet. Sci.* **37**, 977–985.
606 Boato G. (1954) The isotopic composition of hydrogen and carbon in the carbonaceous
607 chondrites. *Geochim. Cosmochim. Acta* **6**, 209–220.
608 Bonal L., Quirico E., Bourot-Denise M. and Montagnac G. (2006) Determination of the
609 petrologic type of CV3 chondrites by Raman spectroscopy of included organic matter.
610 *Geochim. Cosmochim. Acta* **70**, 1849–1863.
611 Brearley A.J. (2006) The action of water. In *Meteorites and the Early Solar System II*, D. S.
612 Lauretta and H. Y. McSween Jr. (eds.), University of Arizona Press, Tucson, 943 pp, pp. 587–
613 624.
614 Busemann H., Young A.F., Alexander C.M.O'D., Hoppe P.; Mukhopadhyay S. and Nittler
615 L.R. (2006) Interstellar Chemistry Recorded in Organic Matter from Primitive Meteorites.
616 *Science* **312**, 727–730.
617 Clog M., Aubaud C., Cartigny P. and Dosso L. (2013) The hydrogen isotopic composition
618 and water content of southern Pacific MORB: A reassessment of the D/H ratio of the
619 depleted mantle reservoir. *Earth Planet. Sci. Lett.* **381**, 156–165.
620 Dauphas N. (2017) The isotopic nature of the Earth's accreting material through time. *Nature*
621 **541**, 521–524.
622 Deloule E. and Robert F. (1995) Interstellar water in meteorites? *Geochim. Cosmochim. Acta*
623 **59**, 4695–4706.

624 Eiler J. M. and Kitchen N. (2004) Hydrogen isotope evidence for the origin and evolution of
625 the carbonaceous chondrites. *Geochim. Cosmochim. Acta* **68**, 1395–1411.
626 Florin G., Luais B., Rushmer T. and Alard O. (2020) Influence of redox processes on the
627 germanium isotopic composition of ordinary chondrites. *Geochim. Cosmochim. Acta* **269**,
628 270–291.
629 Frankenberg C., Yoshimura K., Warneke T., Aben I., Butz A., Deutscher N., Griffith D., Hase
630 F., Notholt J., Schneider M., Schrijver H. and Rockmann T. (2009) Dynamic Processes
631 Governing Lower-Tropospheric HDO/H_2O Ratios as Observed from Space and Ground.
632 *Science* **325**, 1374–1377.
633 Ganino C. and Libourel G. (2017) Reduced and unstratified crust in CV chondrite parent
634 body. *Nature Communications*, 1–10.
635 Garenne A., Beck P., Montes-Hernandez G., Chiriac R., Toche F., Quirico E., Bonal L. and
636 Schmitt B. (2014) The abundance and stability of "water" in type 1 and 2 carbonaceous
637 chondrites (CI, CM and CR). *Geochim. Cosmochim. Acta* **137**, 93–112.
638 Gaudin A., Ansan V. and Rigaudier T. (2015) Mineralogical and δ18O–δD isotopic study of
639 kaolinized micaschists at Penestin, Armorican Massif, France: New constraint in the
640 kaolinization process. *CATENA* **133**, 97–106.
641 Geiss J and Gloeckler G (2003) Isotopic composition of H, He and Ne in the protosolar cloud.
642 *Space Science Reviews* **106**, 3–18.
643 Gilmour C. M., Herd C. D. K. and Beck P. (2019) Water abundance in the Tagish Lake
644 meteorite from TGA and IR spectroscopy: Evaluation of aqueous alteration. *Meteorit.*
645 *Planet. Sci.* **54**, 1951–1972.
646 Girard J.-P., Freyssinet P. and Chazot G. (2000) Unraveling climatic changes from
647 intraprofile variation in oxygen and hydrogen isotopic composition of goethite and
648 kaolinite in laterites: an integrated study from Yaou, French Guiana. *Geochim.*

649 *Cosmochim. Acta* **64**, 409–426.
650 Gong B., Zheng Y.-F. and Chen R.-X. (2007) TC/EA-MS online determination of hydrogen
651 isotope composition and water concentration in eclogitic garnet. *Phys Chem Minerals* **34**,
652 687–698.
653 Gounelle M., Engrand C., Alard O., Bland P. A., Zolensky M. E., Russell S. S. and Duprat J.
654 (2005) Hydrogen isotopic composition of water from fossil micrometeorites in howardites.
655 *Geochim. Cosmochim. Acta* **69**, 3431–3443.
656 Grossman J. N., Alexander C. M. O.'D., Wang J. and Brearley A. J. (2000) Bleached
657 chondrules: Evidence for widespread aqueous processes on the parent asteroids of ordinary
658 chondrites. *Meteorit. Planet. Sci.* **35**, 467–486.
659 Haack H., Grau T., Bischoff A., Horstmann M., Wasson J., Sørensen A., Laubenstein M., Ott
660 U., Palme H., Gellisen M., Greenwood R. C., Pearson V. K., Franchi I. A., Gabelica Z. and
661 Schmitt-kopplin P. (2012) Maribo—A new CM fall from Denmark. *Meteorit. Planet. Sci.*
662 **47**, 30–50.
663 Howard K. T., Alexander C. M. O.'D., Schrader D. L. and Dyl K. A. (2015) Classification of
664 hydrous meteorites (CR, CM and C2 ungrouped) by phyllosilicate fraction: PSD-XRD
665 modal mineralogy and planetesimal environments. *Geochim. Cosmochim. Acta* **149**, 206–
666 222.
667 Howard K. T., Benedix G. K., Bland P. A. and Cressey G. (2010) Modal mineralogy of CV3
668 chondrites by X-ray diffraction (PSD-XRD). *Geochim. Cosmochim. Acta* **74**, 5084–5097.
669 Huss G. R., Rubin A. E. and Grossman J. N. (2006) Thermal Metamorphism in Chondrites. In
670 *Meteorites and the Early Solar System II*, D. S. Lauretta and H. Y. McSween Jr. (eds.),
671 University of Arizona Press, Tucson, 943 pp, pp. 567–586.
672 Kerridge J. F. (1985) Carbon, hydrogen and nitrogen in carbonaceous chondrites: Abundances
673 and isotopic compositions in bulk samples. *Geochim. Cosmochim. Acta* **49**, 1707–1714.

674 King A. J., Bates H.C., Krietsch D., Busemann H., Clay P.L., Schofield P.F. and Russell S.S.
675 (2019a) The Yamato-type (CY) carbonaceous chondrite group: Analogues for the surface
676 of asteroid Ryugu? *Geochemistry* **79**, 125531.
677 King A. J., Russell S. S., Schofield P. F., Humphreys- Williams E. R., Strekopytov S.,
678 Abernethy F. A. J., Verchovsky A. B. and Grady M. M. (2019b) The alteration history of
679 the Jbilet Winselwan CM carbonaceous chondrite: An analog for C- type asteroid sample
680 return. *Meteorit. Planet. Sci.*, 521–543.
681 King A. J., Schofield P. F., Howard K. T. and Russell S. S. (2015) Modal mineralogy of CI
682 and CI-like chondrites by X-ray diffraction. *Geochim. Cosmochim. Acta* **165**, 148–160.
683 Kolodny Y., Kerridge J. F. and Kaplan I. R. (1980) Deuterium in carbonaceous chondrites.
684 *Earth Planet. Sci. Lett.* **46**, 149–158.
685 Krot A. N., Petaev M. I. and Bland P. A. (2004) Multiple formation mechanisms of ferrous
686 olivine in CV carbonaceous chondrites during fluid-assisted metamorphism. *Antarctic*
687 *Meteorite Research* 17, 153-171.
688 Kruijer T. S., Burkhardt C., Budde G. and Kleine T. (2017) Age of Jupiter inferred from the
689 distinct genetics and formation times of meteorites. *Proceedings of the National Academy*
690 *of Sciences*, 201704461.
691 Lécuyer C., Gillet P. and Robert F. (1998) The hydrogen isotope composition of seawater and
692 the global water cycle. *Chem. Geol.* **145**, 249–261.
693 Lindgren P., Lee M. R., Sofe M. R. and Zolensky M. E. (2013) Clasts in the CM2
694 carbonaceous chondrite Lonewolf Nunataks 94101: Evidence for aqueous alteration prior
695 to complex mixing. *Meteorit. Planet. Sci.***48**, 1074–1090.
696 Lodders K. (2003) Solar system abundances and condensation temperatures of the elements.
697 *The Astrophysical J.* **591**, 1220–1247.
698 Lupker M., France-Lanord C., Galy V., Lavé J., Gaillardet J., Gajurel A. P., Guilmette C.,

Rahman M., Singh S. K. and Sinha R. (2012) Predominant floodplain over mountain weathering of Himalayan sediments (Ganga basin). *Geochim. Cosmochim. Acta* **84**, 410–432.

Marrocchi Y., Bekaert D. V. and Piani L. (2018) Origin and abundance of water in carbonaceous asteroids. *Earth Planet. Sci. Lett.* **482**, 23–32.

Marty B. (2012) The origins and concentrations of water, carbon, nitrogen and noble gases on Earth. *Earth Planet. Sci. Lett.* **313–314**, 56–66.

Marty B., Avice G., Sano Y., Altwegg K., Balsiger H., Hässig M., Morbidelli A., Mousis O. and Rubin M. (2016) Origins of volatile elements (H, C, N, noble gases) on Earth and Mars in light of recent results from the ROSETTA cometary mission. *Earth Planet. Sci. Lett.* **441**, 91–102.

McCubbin F. M. and Barnes J. J. (2019) Origin and abundances of H2O in the terrestrial planets, Moon, and asteroids. *Earth Planet. Sci. Lett.* **526**, 115771.

McNaughton N. J., Fallick A. E. and Pillinger C. T. (1982) Deuterium enrichments in type 3 ordinary chondrites. *J. Geophys. Res.* **87**, A297.

Morbidelli A., Chambers J., Lunine J. I., Petit J. M., Robert F., Valsecchi G. B. and Cyr K. E. (2000) Source regions and timescales for the delivery of water to the Earth. *Meteorit. Planet. Sci.* **35**, 1309–1320.

Nanne J. A. M., Nimmo F., Cuzzi J. N. and Kleine T. (2019) Origin of the non-carbonaceous–carbonaceous meteorite dichotomy. *Earth Planet. Sci. Lett.* **511**, 44–54.

Pearson V.K., Sephton M.A., Gilmour I and Franchi I.A. (2001) Hydrogen isotopic composition of the Tagish Lake meteorite: Comparison with other carbonaceous chondrites. In Lunar and Planetary Science. Houston. p. 1861.

Piani L. and Marrocchi Y. (2018) Hydrogen isotopic composition of water in CV-type carbonaceous chondrites. *Earth Planet. Sci. Lett.* **504**, 64–71.

724 Piani L., Marrocchi Y., Vacher L. G., Piralla M., Bizzarro M., Alexander C. M. O.'D.,
725 Howard K. T. and de Lorraine U. (2019) Hydrogen isotopic composition of water in
726 hydrated chondrites. 82th meeting of the Meteoritical Society Meeting, Sapporo, Japan,
727 abstract # 2159.
728 Piani L., Robert F. and Remusat L. (2015) Micron-scale D/H heterogeneity in chondrite
729 matrices: A signature of the pristine solar system water? *Earth Planet. Sci. Lett.* **415**, 154–
730 164.
731 Piani L., Yurimoto H. and Remusat L. (2018) A dual origin for water in carbonaceous
732 asteroids revealed by CM chondrites. *Nature Astronomy*, 1–7.
733 Pizzarello S., Feng X., Epstein S. and Cronin J.R. Isotopic analyses of nitrogenous
734 compounds from the Murchison meteorite: ammonia, amines, amino acids, and polar
735 hydrocarbons. *Geochim. Cosmochim. Acta* **58**, 5579-5587.
736 Pizzarello S., Cooper G.W. and Flynn G.J. (2006) The Nature and Distribution of the Organic
737 Material in Carbonaceous Chondrites and Interplanetary Dust Particles. In *Meteorites and*
738 *the Early Solar System II*, D. S. Lauretta and H. Y. McSween Jr. (eds.), University of
739 Arizona Press, Tucson, 943 pp, p.625-651
740 Protin M., Blard P.-H., Marrocchi Y. and Mathon F. (2016) Irreversible adsorption of
741 atmospheric helium on olivine: A lobster pot analogy. *Geochim. Cosmochim. Acta* **179**,
742 76–88.
743 Raymond S. N. and Izidoro A. (2017) Origin of water in the inner Solar System:
744 Planetesimals scattered inward during Jupiter and Saturn's rapid gas accretion. *Icarus* **297**,
745 134-148.
746 Remusat L., Bonnet J.-Y., Bernard S., Buch A. and Quirico E. (2019) Molecular and isotopic
747 behavior of insoluble organic matter of the Orgueil meteorite upon heating. *Geochim.*
748 *Cosmochim. Acta* **263**, 235–247.

749 Remusat L., Piani L. and Bernard S. (2016) Thermal recalcitrance of the organic D-rich
750 component of ordinary chondrites. *Earth Planet. Sci. Lett.* **435**, 36–44.
751 Robert F. and Epstein S. (1982) The concentration and isotopic composition of hydrogen,
752 carbon and nitrogen in carbonaceous meteorites. *Geochim. Cosmochim. Acta* **46**, 81–95.
753 Robert F. (1978) Teneur en eau et en deuterium des chondrites. Ph. D. thesis. Univ. Paris 7.
754 Robert F., Merlivat L. and Javoy M. (1979) Deuterium concentration in the early Solar
755 System: hydrogen and oxygen isotope study. *Nature* **282**, 785–789.
756 Robert, F. (2003) The D/H ratio in chondrites. *Space Sci. Rev.***106**, 87-101.
757 Rubin A. E. (2005) Relationships among intrinsic properties of ordinary chondrites:
758 Oxidation state, bulk chemistry, oxygen-isotopic composition, petrologic type, and chondrule
759 size. *Geochim. Cosmochim. Acta* **69**, 4907–4918.
760 Rudraswami N. G., Naik A. K., Tripathi R. P., Bhandari N., Karapurkar S. G., Prasad M. S.,
761 Babu E. V. S. S. K. and Sarathi U. V. R. V. (2019) Chemical, isotopic and amino acid
762 composition of Mukundpura CM2.0 (CM1) chondrite: Evidence of parent body aqueous
763 alteration. *Geoscience Frontiers* **10**, 495–504.
764 Salisbury J. W., D'Aria D. M. and Jarosewich E. (1991) Midinfrared (2.5-13.5/ m)
765 Reflectance Spectra. *Icarus*, 280–297.
766 Savin S. M. and Epstein S. (1970) The oxygen and hydrogen isotope geochemistry of clay
767 minerals. *Geochim. Cosmochim. Acta* **34**, 25–42.
768 Smrekar S. E. and Sotin C. (2012) Constraints on mantle plumes on Venus: Implications for
769 volatile history. *Icarus* **217**, 510–523.
770 Stephant A., Garvie L. A. J., Mane P., Hervig R. and Wadhwa M. (2018) Terrestrial exposure
771 of a fresh Martian meteorite causes rapid changes in hydrogen isotopes and water
772 concentrations. *Sci Rep* **8**, 12385.

773 Sutton S., Alexander C. M. O., Bryant A., Lanzirotti A., Newville M. and Cloutis E. A.
774 (2017) The bulk valence state of Fe and the origin of water in chondrites. *Geochim.*
775 *Cosmochim. Acta* **211**, 115–132.
776 Tait A. W., Tomkins A. G., Godel B. M., Wilson S. A. and Hasalova P. (2014) Investigation
777 of the H7 ordinary chondrite, Watson 012: Implications for recognition and classification of
778 Type 7 meteorites. *Geochim. Cosmochim. Acta* **134**, 175–196.
779 Taylor, G.J. (2013) The bulk composition of Mars. *Chemie der Erde - Geochemistry* 73, 401–
780 420.
781 Tomeoka, K., & Buseck, P. R. (1988) Matrix mineralogy of the Orgueil CI carbonaceous
782 chondrite. *Geochim. Cosmochim. Acta* ***52***, 1627−1640.
783 Vacher L. G., Marrocchi Y., Verdier-Paoletti M. J., Villeneuve J. and Gounelle M. (2016)
784 Inward radial mixing of interstellar Water ices in the solar protoplanetary disk. *The*
785 *Astrophysical Journal Letters* **827**, 1–6.
786 Warren P. H. (2011) Stable-isotopic anomalies and the accretionary assemblage of the Earth
787 and Mars: A subordinate role for carbonaceous chondrites. *Earth Planet. Sci. Lett.* **311**,
788 93–100.
789 Yamashita Y. and Naraoka H. (2014) Two homologous series of alkylpyridines in the
790 Murchison meteorite. *Geochemical J.* 48, 519-525.
791 Yang J. and Epstein S. (1983) Interstellar organic matter in meteorites. *Geochim. Cosmochim.*
792 *Acta* **47**, 2199–2216.
793
794
795
796
797

798 **Figure captions**

799

800 Fig. 1. Schematic representation of the analytical protocol used in this study. The samples
801 were first degassed under vacuum at 120 °C for 48 h in a degassing canister (A) before being
802 transferred into a sealed auto-sampler pre-flushed with He (B). Samples were combusted at
803 1450 °C (C) and the extracted H_2 was introduced into the mass spectrometer through an open
804 split and its D/H isotopic composition analyzed (D).

805

806 Fig. 2. (A) Average bulk hydrogen and water abundances (wt.%) for the different groups of
807 chondrites analyzed in this study. Half-filled markers and unfilled triangle represent samples
808 presumably affected by terrestrial weathering and/or metamorphism dehydration (Jbilet
809 Winselwan, Y-980115 and Gro 95502). (B) Distribution of the H isotopic compositions (bulk
810 D/H ratios and equivalent δD values) of chondrites (n = 178). The upper part of the graph
811 presents the H isotopic compositions measured in this study for each group of chondrites, and
812 the lower part presents values reported in literature: Boato (1954), Robert (1978), Robert et al.
813 (1979), Kolodny et al. (1980), Kerridge (1985), McNaughton et al. (1982), Robert and
814 Epstein (1982), Yang and Epstein (1983), Robert (2003), Pearson et al. (2001), and Alexander
815 et al. (2012).

816

817 Fig. 3. Relationship between bulk carbon and nitrogen abundances (wt.%) for all chondrites
818 analyzed. A positive trend (solid black line) is observed between the two parameters, with an
819 R^2 value of 0.77 (MSWD = 1.7). Dashed curves represent the 95% confidence interval of the
820 regression (errors are 2σ).

821

Fig. 4. Bulk hydrogen abundances (expressed as 1/H) and D/H isotopic ratios of CM chondrites and the ungrouped Tagish Lake chondrite ('TL') from this study and Alexander et al. (2012) and CM Paris (Vacher et al., 2016). Two positive trends (solid lines) with distinct slopes but similar intercepts are observed for our data (red; D/H = 70 (± 17) × 1/H + 60 (± 24); 2σ, R^2 = 0.91, MSWD = 21) and the data from Alexander et al. (2012), excluding heated CMs (gray; D/H = 133 (± 28) × 1/H + 28 (± 26); 2σ, R^2 = 0.55, MSWD = 466). Dashed curves represent the 95% confidence intervals of the regressions (errors are 2σ).

Fig. 5. The effect of pre-degassing temperature on the measured (A, B) hydrogen abundances and (C, D) hydrogen isotopic compositions of CM Murchison (red) and CI Orgueil (orange). Measured hydrogen concentrations decrease and D/H ratios increase with increased pre-degassing temperature for Orgueil. Ranges of D/H values of D-rich organic matter (dark gray area; Alexander et al., 2007), D-poor phyllosilicates (light gray area; Alexander et al., 2012; Piani et al., 2018, 2019) and terrestrial hydrosphere (blue area; Lécuyer et al., 1998; Frankenberg et al., 2009; Clog et al., 2013) are also represented for comparison. Data from: Boato (1954), Kolodny et al. (1980), Robert and Epstein ('R&E', 1982), Yang and Epstein ('Y&E', 1983), Pearson et al. (2001), and Alexander et al. (2012).

Fig. 6. The amount of H lost during the pre-degassing procedure as a function of the indigenous H content measured in CV-, CM-, and CI-type carbonaceous chondrites after pre-degassing at 120 °C. The amount of pre-degassed H is calculated as the difference between the hydrogen content measured in our samples after pre-degassing at 120 °C and that measured in the same samples at room temperature (25 °C) using the same analytical technique, but without pre-degassing (Pearson et al., 2001; Alexander et al., 2012) (errors are 2σ).

Fig. 7. Bulk D/H ratios as a function of bulk hydrogen abundances (expressed as 1/H) for all reported analyses of (A) CV chondrites (this study; Boato, 1954; Robert and Epstein, 1982; Kerridge, 1985; Pearson et al., 2001; Alexander et al., 2012) and (B) ordinary chondrites (this study; Robert et al., 1979; McNaughton et al., 1982; Yang and Epstein, 1983; Alexander et al., 2012) (errors are 2σ).

Fig. 8. Bulk hydrogen isotopic compositions of CV (black) and CM (red) chondrites as a function of their bulk C/H ratios. Delta notation is used for H isotopic compositions to facilitate comparison with Alexander et al. (2012). Solid lines and dashed curves represent data regressions and their 95% confidence intervals, respectively (errors are 2σ).

865

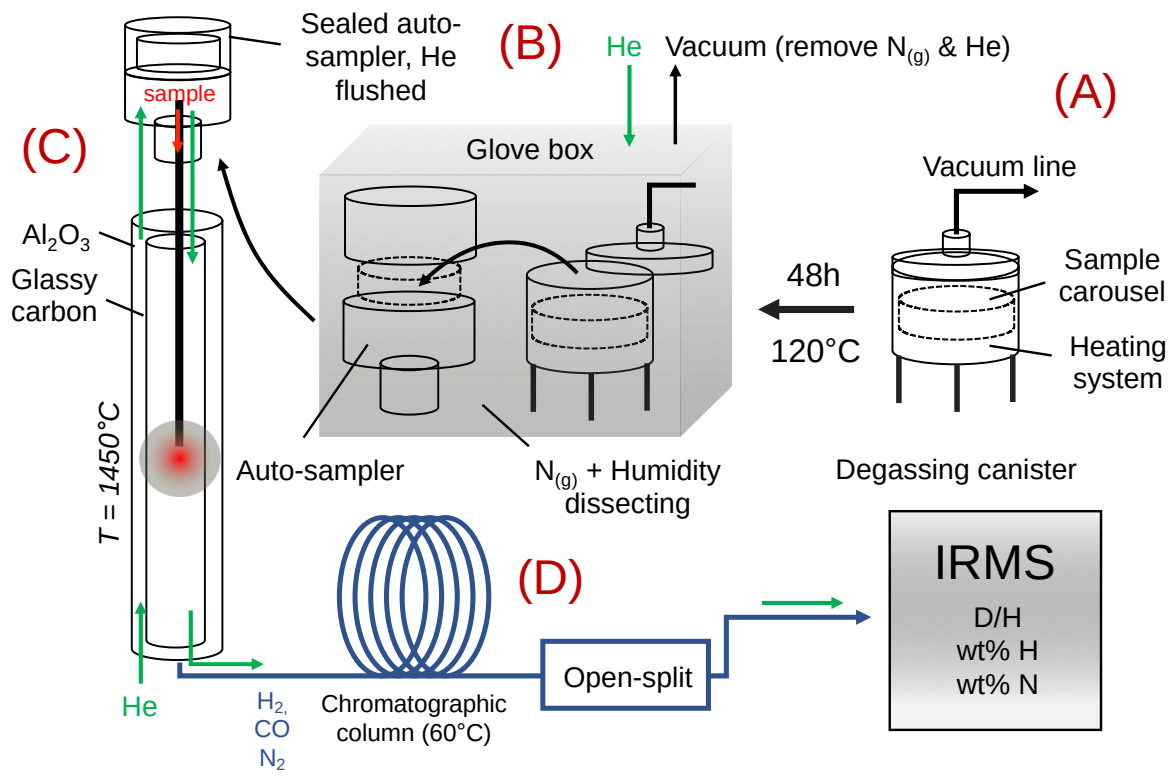

866

867 Fig. 1

868

869

870

871

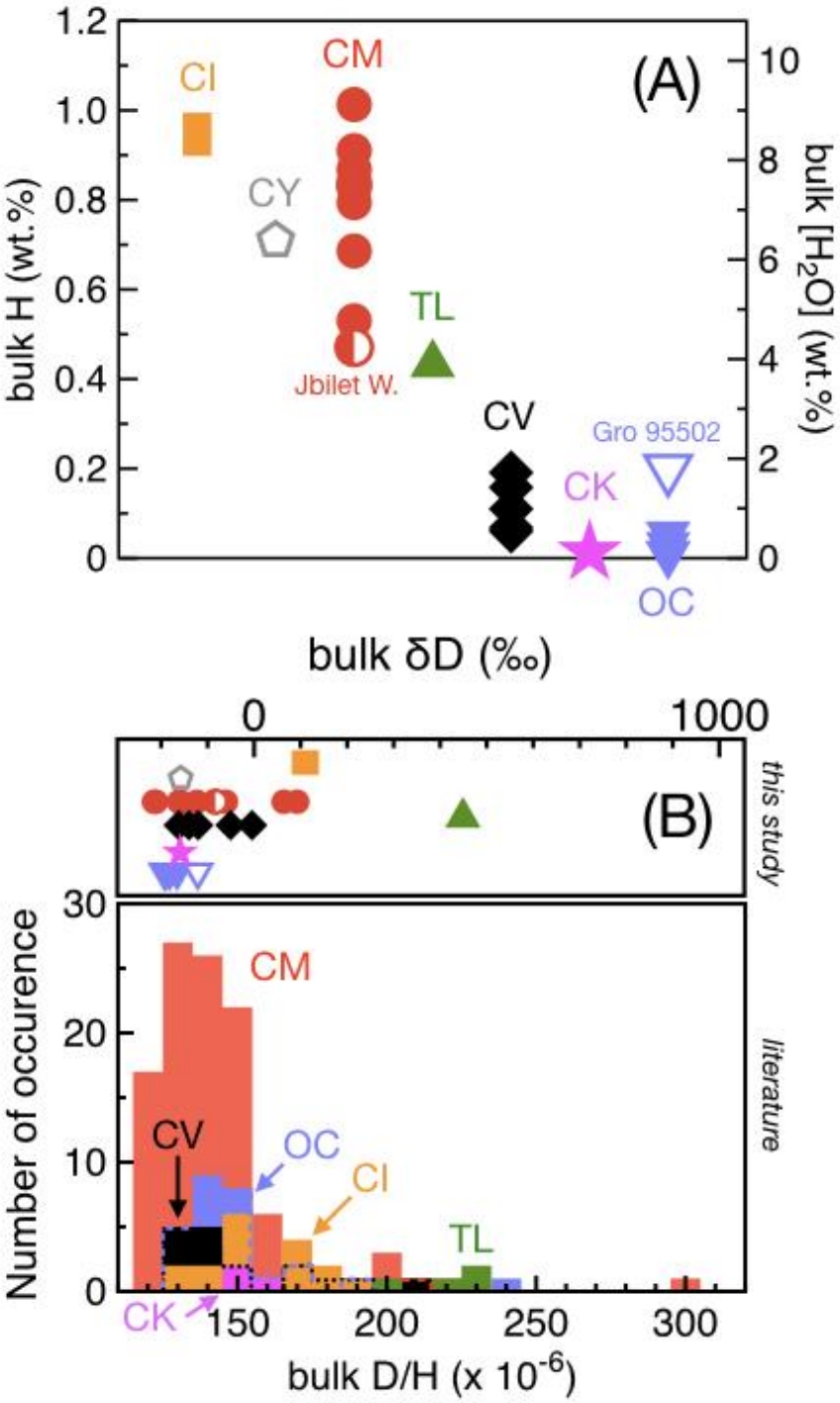
(A)
CI
CM
CY
TL
Jbilet W.
CV
Gro 95502
CK
OC
bulk H (wt.%)
bulk [H2O] (wt.%)
bulk δD (‰)
0
1000
(B)
this study
literature
Number of occurence
CM
CV
OC
CI
TL
CK
150
200
250
300
bulk D/H (x 10-6)

Fig. 2

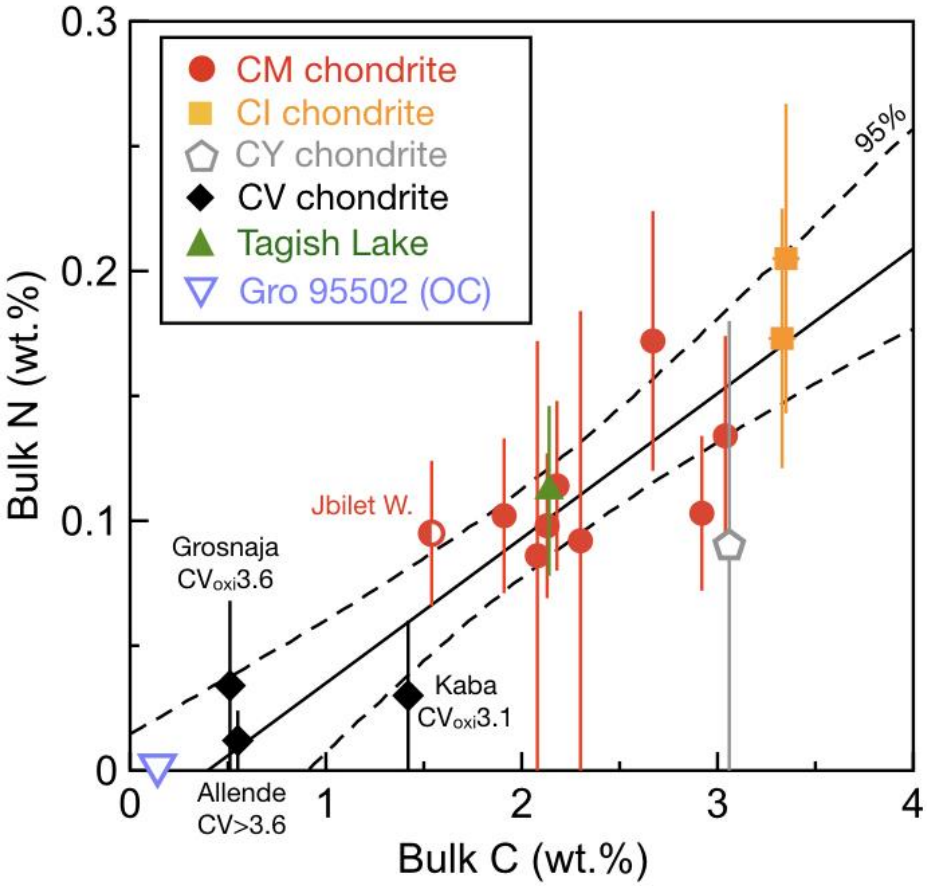
CM chondrite
CI chondrite
CY chondrite
CV chondrite
Tagish Lake
Gro 95502 (OC)
95%
Jbilet W.
Grosnaja
CVoxi3.6
Kaba
CVoxi3.1
Allende
CV>3.6
Bulk N (wt.%)
Bulk C (wt.%)
0.3
0.2
0.1
0
0
1
2
3
4

Fig. 3

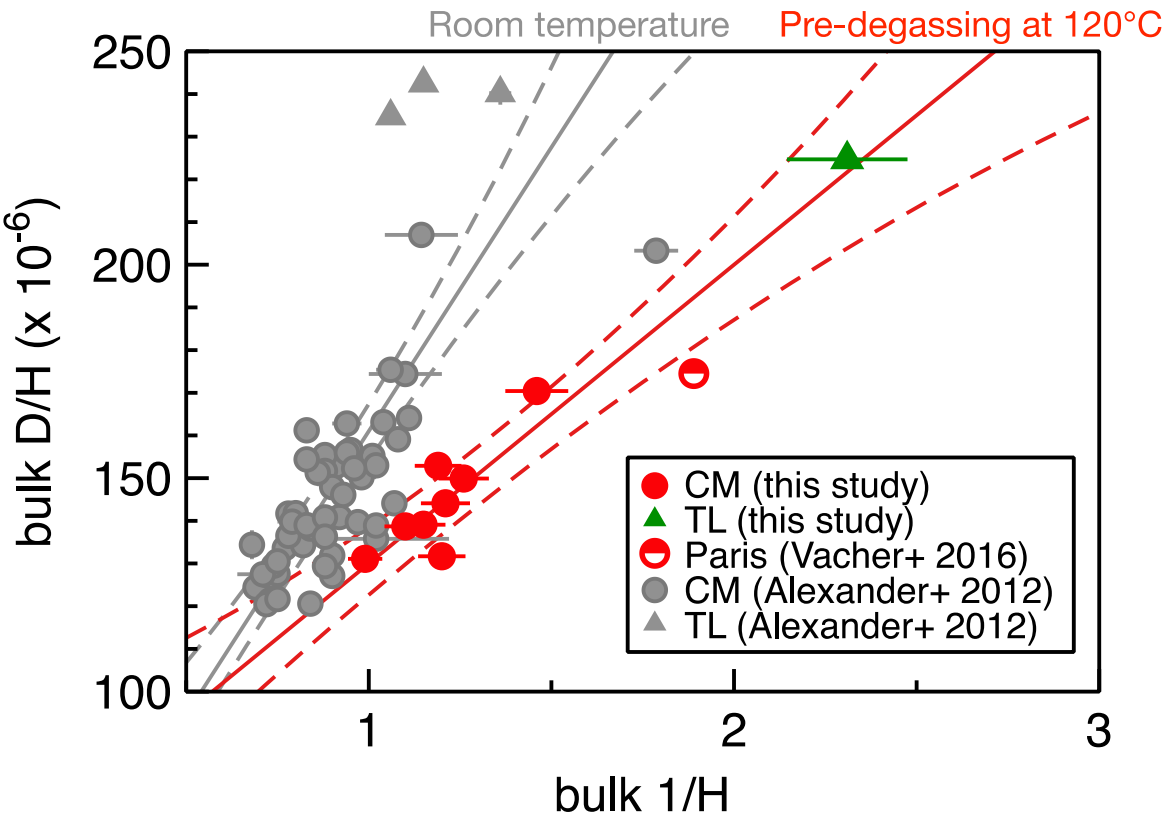
Room temperature
Pre-degassing at 120°C
250
200
150
100
bulk D/H (x 10-6)
1
2
3
bulk 1/H
CM (this study)
TL (this study)
Paris (Vacher+ 2016)
CM (Alexander+ 2012)
TL (Alexander+ 2012)

Fig. 4

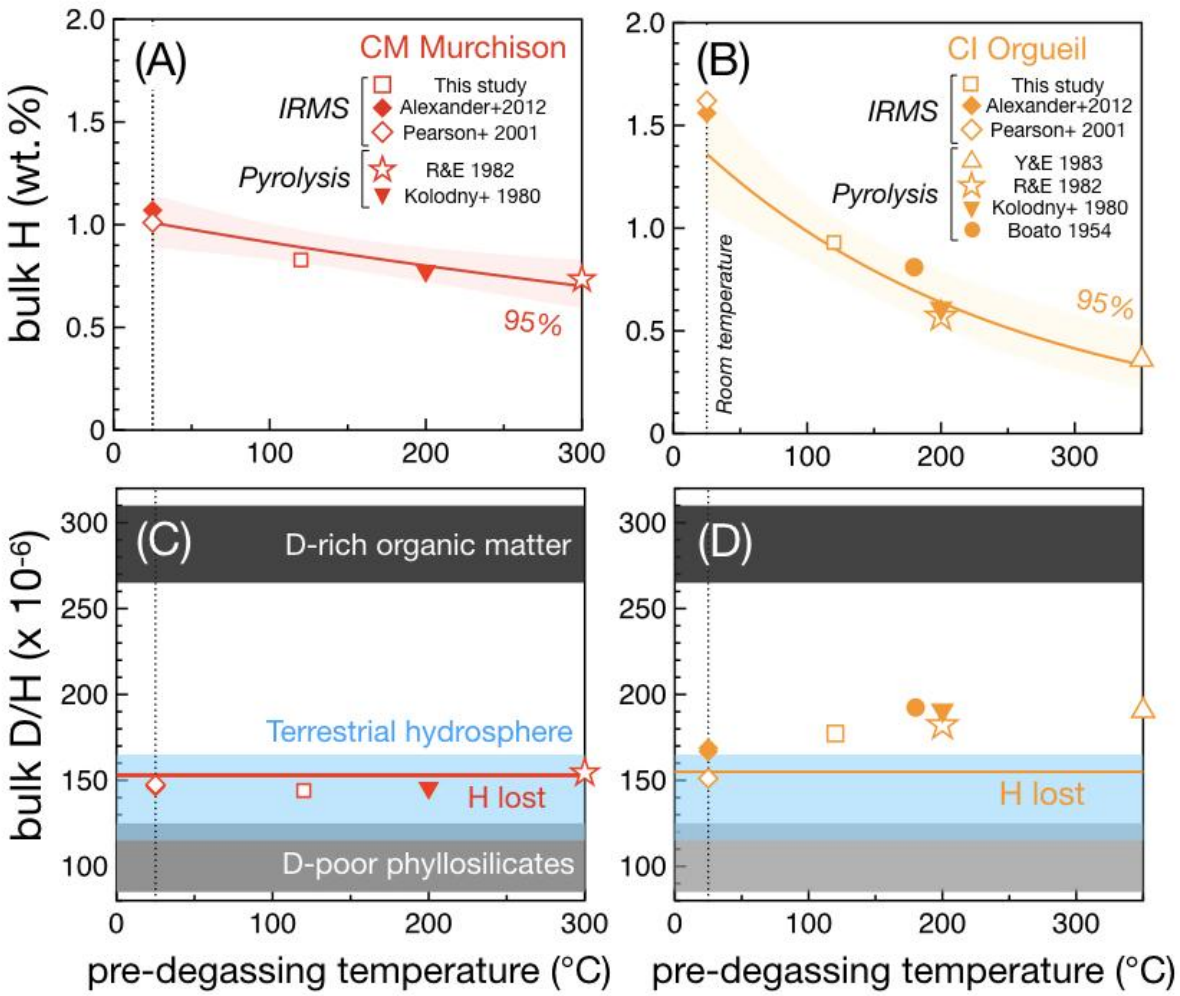
(A)
CM Murchison
IRMS
This study
Alexander+2012
Pearson+ 2001
Pyrolysis
R&E 1982
Kolodny+ 1980
95%
bulk H (wt.%)
(B)
CI Orgueil
IRMS
This study
Alexander+2012
Pearson+ 2001
Pyrolysis
Y&E 1983
R&E 1982
Kolodny+ 1980
Boato 1954
95%
Room temperature
(C)
D-rich organic matter
Terrestrial hydrosphere
H lost
D-poor phyllosilicates
bulk D/H (x 10-6)
pre-degassing temperature (°C)
(D)
H lost
pre-degassing temperature (°C)

Fig. 5

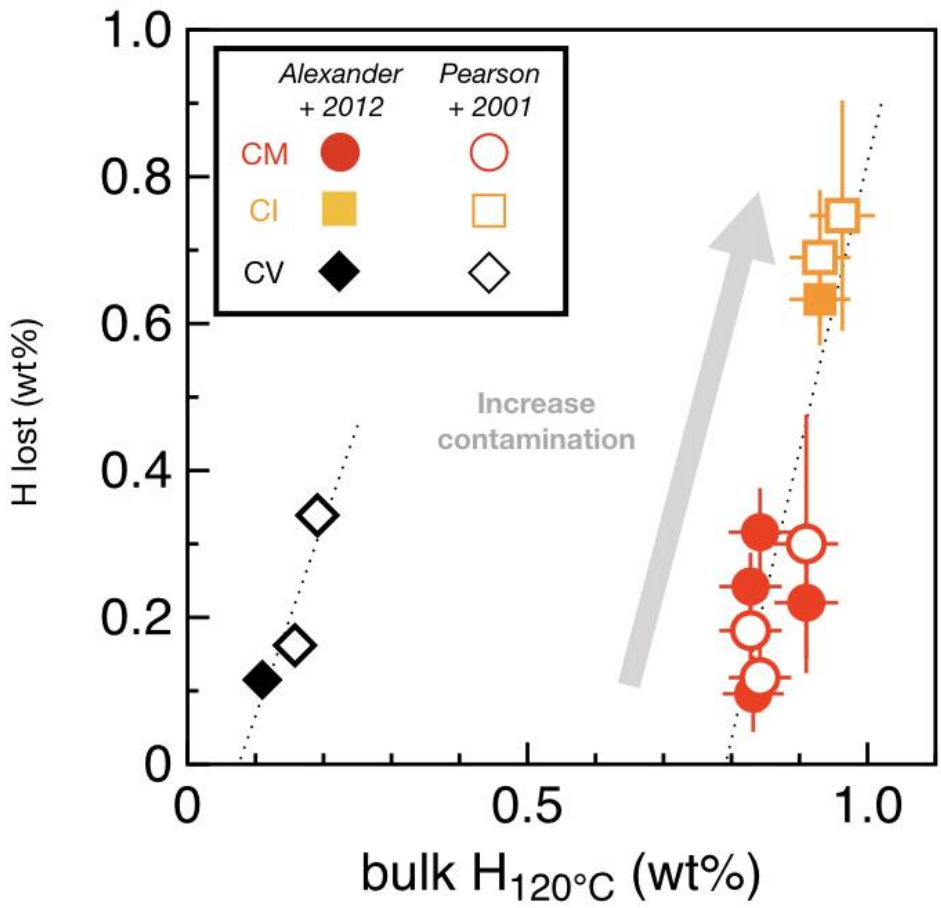
Alexander + 2012
Pearson + 2001
CM
CI
CV
Increase contamination
H lost (wt%)
bulk $H_{120°C}$ (wt%)
0
0.2
0.4
0.6
0.8
1.0
0
0.5
1.0

Fig. 6

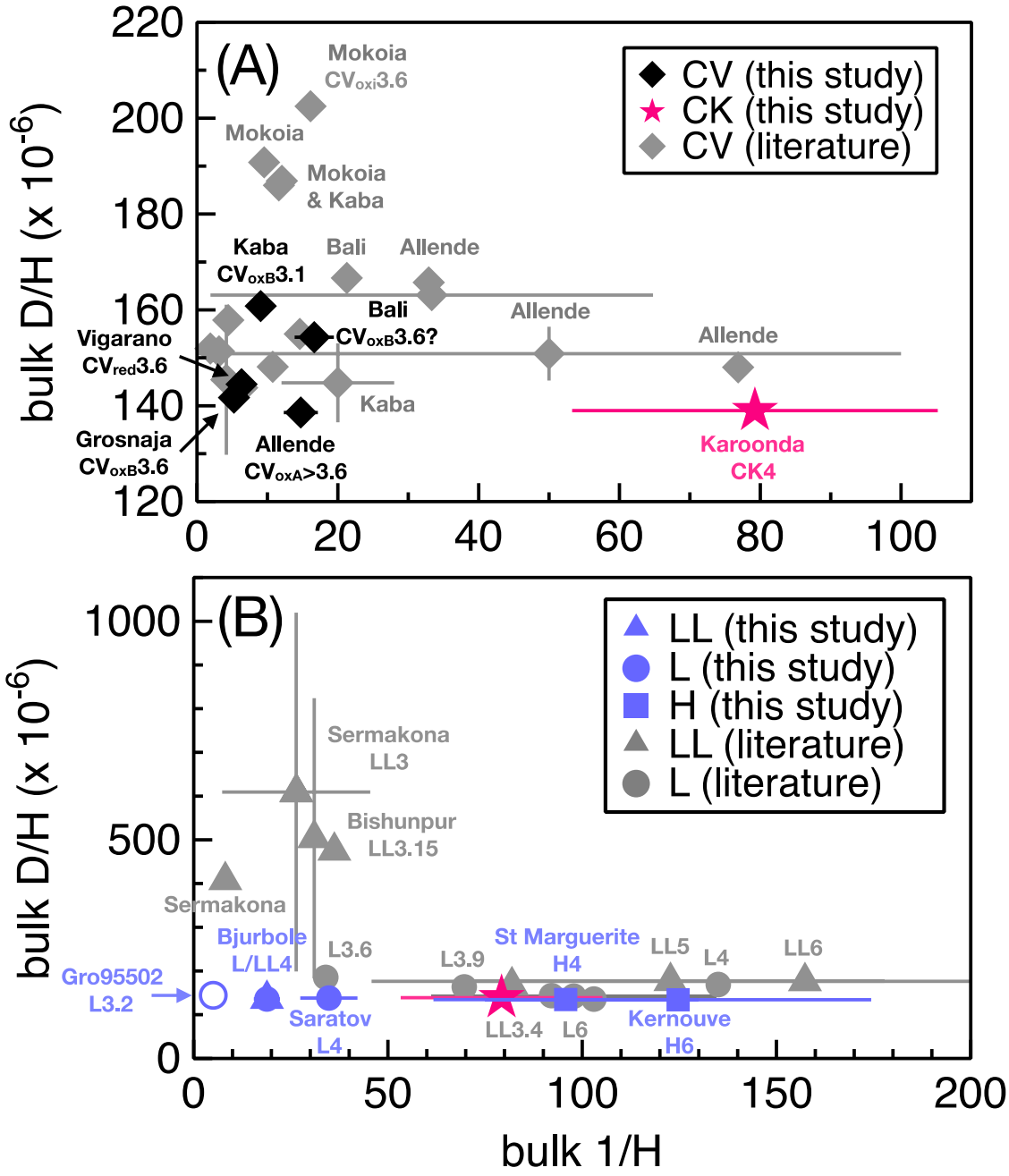
(A)
CV (this study)
CK (this study)
CV (literature)
bulk D/H (x 10-6)
Mokoia
CVoxi3.6
Mokoia
Mokoia
& Kaba
Kaba
CVoxB3.1
Bali
Allende
Bali
CVoxB3.6?
Allende
Allende
Vigarano
CVred3.6
Kaba
Grosnaja
CVoxB3.6
Allende
CVoxA>3.6
Karoonda
CK4
220
200
180
160
140
120
0
20
40
60
80
100
(B)
LL (this study)
L (this study)
H (this study)
LL (literature)
L (literature)
bulk D/H (x 10-6)
Sermakona
LL3
Bishunpur
LL3.15
Sermakona
Bjurbole
L/LL4
L3.6
St Marguerite
H4
L3.9
LL5
L4
LL6
Gro95502
L3.2
Saratov
L4
LL3.4
L6
Kernouve
H6
1000
500
0
0
50
100
150
200
bulk 1/H

Fig. 7

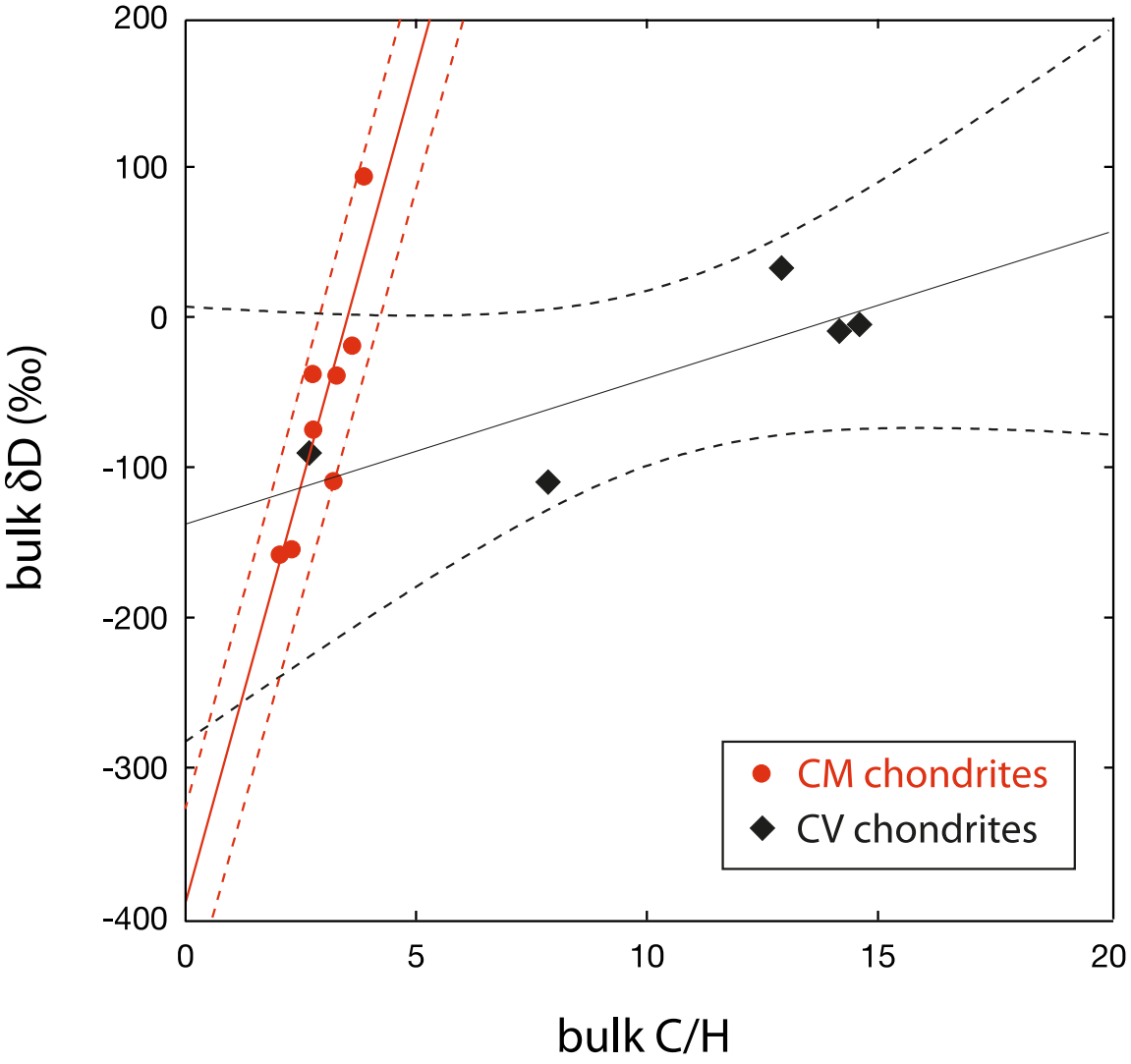
200
100
0
-100
-200
-300
-400
bulk δD (‰)
0
5
10
15
20
bulk C/H
CM chondrites
CV chondrites

Fig. 8

Table 1: Hydrogen abundances and isotopic compositions of chondrites.

Meteorite	Type	wt% H	err. (2σ)	2 sd	δD (‰)	err. (2σ)	2 sd	D/H ($\times10^{-6}$)	err. (2σ)	2 sd
Aguas Zarcas (*n* =2)	CM2	0.868	0.045	0.087	-107.1	2	1.6	139.1	0.3	0.3
Jbilet Winselwan (*n* = 2)	CM2	0.471	0.032	0.018	-38.9	2	9.5	149.7	0.3	1.5
LON 94101 (*n* = 2)[c]	CM2	0.832	0.045	0.012	-154.6	2	3.1	131.7	0.3	0.5
Maribo (*n* = 2)	CM2	0.794	0.044	0.028	-37.9	2	1.1	149.9	0.3	0.2
Mighei (*n* = 2)	CM2	0.910	0.047	0.038	-109.4	2	0.8	138.7	0.3	0.1
Mukundpura (*n* = 4)	CM2	1.013	0.048	0.139	-158.2	2	6.7	131.1	0.3	1
Murchison (*n* = 2)	CM2	0.828	0.046	0.081	-74.9	2	0.9	144.1	0.3	0.1
Murray (*n* = 2)	CM2	0.842	0.046	0.038	-18.5	2	2.6	152.9	0.3	0.4
Paris (altered area)[a]	CM2	0.686	0.040		93.7	2		170.4	0.3	
Paris[b]	CM2	0.530	0.010		120.3	1		174.5	0.3	
Tagish Lake (*n* = 3)	Ung. C	0.433	0.031	0.007	442.3	2	24	224.7	0.3	3.7
Alais (*n* = 2)	CI	0.963	0.048	0.092	133.7	2	28.9	176.6	0.3	4.5
Orgueil (*n* = 4)	CI	0.930	0.045	0.148	138.0	2	15.3	177.3	0.3	2.4
Y-980115 (*n* = 3)[d]	CY	0.710	0.041	0.212	-106.0	2	3	139.2	0.3	0.5
Allende (*n* = 2)	CV	0.068	0.011	0.011	-109.9	2	2.4	138.6	0.8	0.4
Bali	CV	0.060	0.010		-9.3	5		154.3	0.8	
Grosnaja	CV	0.191	0.019		-90.5	5		141.7	0.8	
Kaba	CV	0.110	0.014		32.6	5		160.8	0.8	
Vigarano	CV	0.158	0.018		-72.6	5		144.5	0.8	
Karoonda	CK	0.013	0.004		-107.4	5		139.0	0.8	
Bjurbole	LL/L4	0.053	0.009		-128.1	5		135.8	0.8	
GRO 95502[e]	L3	0.199	0.020		-73.2	5		144.4	0.8	
Saratov (*n* = 2)	L4	0.029	0.006	0.011	-113.7	5	2.3	138.1	0.8	0.4
Sainte Marguerite	H4	0.010	0.004		-135.8	5		134.6	0.8	
Kernouve	H6	0.008	0.003		-138.3	5		134.2	0.8	

[a]Piece of Paris provided by Bekaert et al. (2018). [b]Data from Vacher et al. (2016) using the same methodology as this study. [c]Lonewolf Nunataks 94101. [d]Yamato 980115. [e]Grosvenor Mountains. Err. (2σ): 2σ sample error (see methods). 2 sd: 2σ standard deviation on *n* replicates.

926 Table 2: Carbon and nitrogen abundances and carbon isotopic compositions of chondrites.
927

Meteorite	Type	wt% N	err. (2σ)	2 sd	wt% C	err. (2σ)	2 sd	$\delta^{13}C$ (‰)	err. (2σ)	2 sd
Aguas Zarcas	CM2	0.098	0.029		2.13	0.04		-9.8	0.2	
Jbilet Winselwan	CM2	0.095	0.029		1.54	0.03		-10.9	0.2	
LON 94101[a]	CM2	0.102	0.031		1.91	0.04		-13.7	0.2	
Maribo	CM2	0.114	0.034		2.18	0.04		-5.5	0.2	
Mighei	CM2	0.103	0.031		2.92	0.06		-12.5	0.2	
Mukundpura (*n* = 3)	CM2	0.086	0.086	0.008	2.08	0.04	0.04	-3.9	0.2	2.3
Murchison	CM2	0.092	0.092		2.30	0.05		-10.4	0.2	
Murray	CM2	0.134	0.040		3.04	0.06		-11.7	0.2	
Paris	CM2	0.172	0.052		2.67	0.05		-7.5	0.2	
Tagish Lake	Ung. C	0.112	0.034		2.14	0.04		4.7	0.2	
Alais	CI	0.173	0.052		3.33	0.07		-15.9	0.2	
Orgueil (*n* = 2)	CI	0.205	0.062	0.014	3.35	0.07	0.78	-12.9	0.2	5.7
Y-980115[b]	CY	0.090	0.090		3.06	0.06		-12.9	0.2	
Allende	CV	0.012	0.012		0.55	0.01		-23.7	0.2	
Bali	CV	bdl			0.85	0.02		-19.9	0.2	
Grosnaja	CV	0.034	0.034		0.51	0.01		-21.6	0.2	
Kaba	CV	0.030	0.030		1.42	0.03		-17.8	0.2	
Vigarano	CV	bdl			bdl			bdl	0.2	
Karoonda	CK	bdl			0.09	0.00		-20.7	0.2	
Bjurbole	LL/L4	bdl			0.14	0.00		-26.5	0.2	
GRO 95502[c]	L3	bdl			bdl			bdl	0.2	
Saratov	L4	bdl			0.12	0.00		-26.2	0.2	
Sainte Marguerite	H4	bdl			0.08	0.00		-24.7	0.2	
Kernouve	H6	bdl			0.10	0.00		-26.6	0.2	

928 [a]Lonewolf Nunataks 94101, [b]Yamato 980115 [c]Grosvenor Mountains.
929 Err. (2σ): 2σ sample error (see methods), 2 sd: 2σ standard deviation on *n* replicates.
930
931
932
933
934
935
936
937
938